Vibration-based Fault Detection System with IoT Capabilities for a Conveyor Machine

Ricardo Martínez-Parrales[1], Adriana del Carmen Téllez-Anguiano[2,*]

[1]DIE, Tecnológico Nacional de México / Instituto Tecnológico de Morelia, Av. Tecnológico 1500, Col. Lomas de Santiaguito, C.P. 58120, Morelia, Michoacán, México, ricardo.mp@morelia.tecnm.mx

[2]DEPI, Tecnológico Nacional de México / Instituto Tecnológico de Morelia, Av. Tecnológico 1500, Col. Lomas de Santiaguito, C.P. 58120, Morelia, Michoacán, México, adriana.ta@morelia.tecnm.mx

*Corresponding author

Abstract: In the industry, the continuous operation of machines is required, making it difficult to stop and carry out preventive maintenance to check the status of the wear elements. However, the early detection of a faulty element allows avoiding further damage to the machine and the user. Thus, it is very important to have continuous and remote monitoring of the machine's status and the wear of its elements without stopping the process; to this aim, vibration analysis is one of the most effective techniques. In this paper, a vibration-based fault detection system with IoT capabilities applied to a vibrating conveyor is presented. The system processes the acceleration force measured in 6 points of the machine using two-axis wireless accelerometers and obtains the position-time date time to derive three machine parameters: stroke, direction and frequency; comparing these values to their nominal reference the system provides a visual interface to inform the operator both, in situ and remotely, the status of the machine. The system performance is validated through a physical conveyor prototype.

Keywords: Vibration analysis; Conveyor machine; Fault detection system; IoT

1 Introduction

Fault detection systems have been widely used in different fields to perform early detection of faults, avoiding damage to the system and the user. Nowadays, several of these detection systems are based on mathematical models of the process to avoid the physical redundancy of actuators and sensors.

In literature, several models and algorithms that adequately represent the behavior of different systems can be found. The analyzed models are not only oriented to

represent industrial systems but also social behaviors, for instance, authors in [1] analyze and identify human activities under uncertain conditions; also, the mathematical analysis of how the seasonal time affects tourism is presented in [2].

Models have also been used in control tasks. In [3], a fuzzy control based on myoelectric signals applied to a prosthetic hand is presented. However, the online implementation of these models can be difficult in industrial processes that require low-cost and physically robust solutions.

In the industry, continuous processes demand more machine uptime making it difficult to stop the machine and to carry out preventive maintenance to check the status of the wear elements.

On the other hand, early detection of a faulty element yields in a replacement of only the failing part avoiding the damage to be spread to other machine parts [4].

This means that it is very important to have a continuous, remote if possible, monitoring of the machine's status and the wear of its elements without having to stop the process. In the case of motor bearings, machine vibration analysis is one of the most effective techniques [4], [5], [6].

The study case in this paper is a vibratory conveyor. A vibratory conveyor achieves the transportation of particles by vibrating at a specified frequency width and specific stroke length and angle [7], [8], such that it is also important to have continuous monitoring of the vibration frequency as well as the direction of these vibrations to detect anomalies in the conveyor's joints.

Moreover, it is important to process the before mentioned information in real-time to indicate to the operator the status of the machine elements to efficiently program the machine preventive maintenance avoiding unnecessary stopping times.

Different vibration analysis techniques and sensing methods have been reported in the literature to detect machine anomalies. In [8], damage detection is observed by tracking the vibration energy distribution over time. An unobtrusive vibration based on optical strobing is presented in [9] whereas a vibration sensing based on optical fibers is presented in [10]. In order to filter the vibrating signal noise, a genetic algorithm is presented in [11].

Different from the above-mentioned proposal, the main contribution of this paper is determining the status of the wear elements in a vibrating conveyor by processing the acceleration force measured at six different points of the machine using two-axis wireless accelerometers, without using complex mathematical models, which in-situ implementation can be difficult in the fault detection system.

Using a low-cost ESP32 microcontroller, the acceleration data is integrated with respect to time to obtain the velocity of the vibration and then integrated to obtain the position over time where three machine parameters are derived: stroke displacement, direction and frequency.

The machine parameters are then compared to the nominal parameters of the machine to obtain a deviation and, by using the technician's expertise, fixed thresholds are defined to translate such deviations into green, yellow or red status for each parameter to continuously inform the operator of the status of the machine.

Moreover, the placement and removal of the sensors can be carried out without stopping the machine's process and with no mechanical or electric connections involved and the selected microcontroller can transmit data using Wi-Fi, enabling remote monitoring and allowing IoT tasks.

The rest of the paper is organized as follows: the vibratory conveyor physics is presented in Section 2; the proposed measurement scheme is presented in Section 3; validation of the measurement scheme is reported in Section 4; lastly, the conclusions are presented in Section 5.

2 Vibrating Conveyor

Bulk solids and particles can be transported by using belts, hoists, trams, etc.; they can be propelled to move by augers, drag paddles, and rotary vanes. Sliding these solids over channels or slats and transporting them pneumatically are some of the options [12].

Induced transport is another alternative achieved through a vibrating action that moves the load [4], even when micromachines are considered [13]. The result is a transport movement that is induced rather than forced, yielding in a smooth movement.

This type of transportation can be carried out by applying a suitable stroke in a specific direction at the frequency required by the material such that the applied vibration inherently reduces friction between parts or particles of the moved material.

The principle of operation is based on finding the natural frequency at which the springs come into resonance, avoiding the use of counterweights and controlling the resonance to avoid damaging the machine.

Once the machine springs are vibrating at their natural frequency, a motor only needs to apply the necessary energy to maintain the amplitude of this vibration.

With this method, different displacement patterns can be obtained, as shown in Figure 1, where the linear displacement achieves the most efficient transport is widely used. In the industry, continuous processes demand more machine uptime making it difficult to stop the machine and to carry out preventive maintenance to check the status of the wear elements.

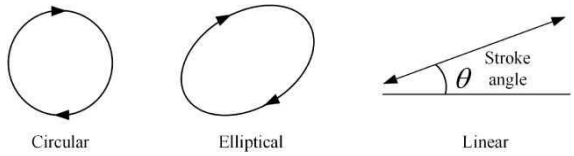

Figure 1
Vibration conveyor movement patterns

Throughout a cycle of linear displacement, shown in Figure 2, the particle separates from the conveyor at point A and begins a free projectile trajectory returning to the conveyor at point C. From point D the particle is pushed in the desired direction.

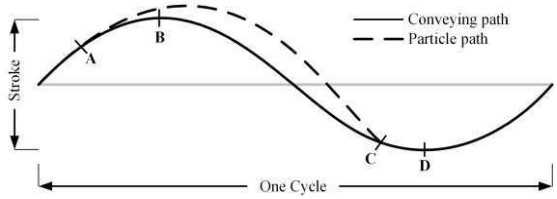

Figure 2
Evolution of the particle throughout a complete cycle of displacement

Depending on the displacement angle, a gentler or more abrupt transport is achieved on the material, obtaining the point with the highest transport speed at 45 degrees, as shown in Figure 3.

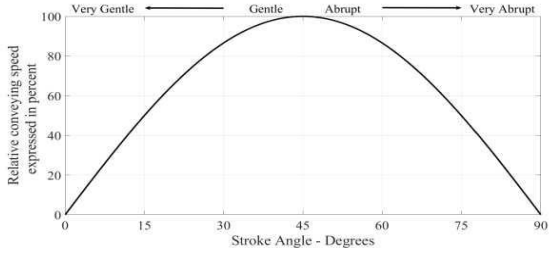

Figure 3
Relationship between the angle and the velocity of the particles.

To obtain a specific displacement angle, it is necessary to define the length of the displacement and the frequency of the vibration based on the characteristics of the material to be transported.

The combination of the length of the displacement and the square of the frequency allows estimating the magnitude of the vibration force, expressed in Gs, necessary to carry out this displacement. Note that different combinations of frequencies and displacement result in a similar G-force.

A short displacement at a high frequency achieves an intense transport at the material surface level with low penetration, which means that only the top layer is transported. On the other hand, a much lower frequency with a greater displacement achieves greater penetration but little movement on the surface. Therefore, each vibration conveyor machine is designed to achieve a specific frequency and displacement.

Knowing these design parameters is feasible to create a motion model of the machine applicable at each point where the resonant springs are located.

In this context, if the vibration, displacement and frequency of the machine are measured at these points, it can be estimated if the machine is operating within the correct expected values or if there is some kind of anomaly or fault.

3 Materials and Methods

The vibration-based fault detection system designed in this work allows determining the operating status of the conveyor by calculating the effective stroke of the machine, as well as its vibration frequency, besides, the ESP32 microcontroller used in its implementation allows including IoT capabilities.

The general scheme of the fault detection system is presented in Figure 4.

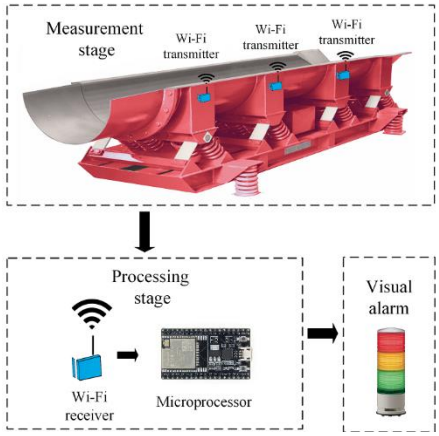

Figure 4
General scheme of the fault detection system

3.1 Vibration Measurement Stage

Different vibration sensors with different accuracies and ranges of measurable G-forces are available in the market. In this work, the Analog Devices ADIS16000 a receiving hub that can manage a wireless sensor network and six ADIS16229 functioning as measurement nodes are selected based on their communication properties, sensibility range and measurement precision.

The ADIS16229 is a wireless vibration sensor node that combines dual-axis acceleration detection with advanced time-domain and frequency-domain signal processing, including the Fast Fourier Transform (FFT) and programmable alarms.

After processing the data from each of the six sensors, a microcontroller must interpret the values to display them numerically to the operator; additionally, the system presents a graphical interface, in the form of a led tower light, which uses the colors: green to indicate a correct operation, yellow for a state that requires attention and red for a fault state.

Furthermore, the selected microcontroller includes a Wi-Fi protocol that allows it to be used as a remote node capable of IoT tasks, such as remote monitoring of the system.

3.1.1. Considerations

The sensors must be self-powered by batteries providing the system with at least 24-hours of autonomy. Data communication must be wireless. The sensors must be placed and removed from the machine without requiring any additional elements, connectors or bolts, and this process must be possible under operating conditions.

The sensor nodes are configured to take constant vibration readings in the 10 Gs range. Since the vibration is measured using an acceleration sensor, conceptually it is possible to integrate such acceleration to obtain the stroke speed and integrate the obtained result to get the stroke.

The theory used to carry out the aforementioned conversions is simple and well known, however, its implementation would only be possible in a noise-free environment, in which the sensor is capable of delivering an accurate acceleration measurement in the direction of the stroke. Because this is not feasible in an industrial operating system, a formulation that considers the characteristics of the sensor and the machine to perform a corrected double integration is required.

First, the sensors are configured such that each value used for the calculation is an average of 10 readings, this is achieved by activating the averaged FFT mode of the ADIS16229, this reduces the Gaussian noise and provides values with an improved signal-to-noise ratio.

The average values are stored in 2 vectors, one corresponding to the X-axis sensor and one corresponding to the Y-axis. These values are scaled according to the configured G range in the ADIS16229.

3.1.2. Frequency and Stroke Estimation Algorithm

Using an ESP32 microcontroller, the data is requested through the SPI port to the ADIS16000 and the proposed 7-step algorithm, presented in Figure 5, is performed in the microcontroller.

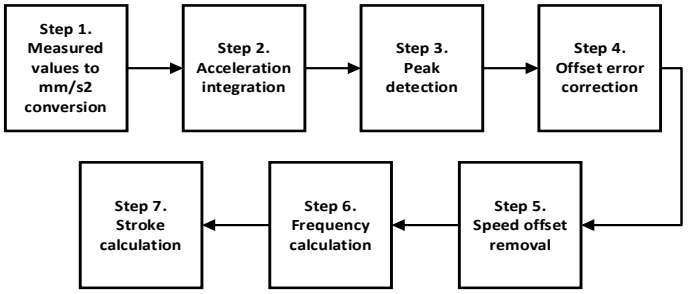

Figure 5
Developed 7-step algorithm to calculate frequency and stroke

Step 1. Convert values to mm/s^2. Values in millimeters per second squared are obtained by converting the measured value according to Eq. (1).

$$aX[i] = aX[i](0.3052)(9.80665), Vi = 0, \ldots, 255 \quad (1)$$

where 9.80665 represents the value of 1 mG in mm/s^2 and 0.3052 is the weight in mGs of the less significant bit (LSB) in the sensor scale of 10 Gs.

Step 2. Integrate the acceleration. A first integration step is performed on the X-axis data using the trapezoidal integration method, as shown in Figure 6, to obtain the velocity on the X-axis according to Eq. (2).

$$\int_a^b f(x)\partial\, x \approx \frac{b-a}{2N}\sum_{n=1}^{N}\left(f(x_n) + f(x_{n+1})\right) \quad (2)$$

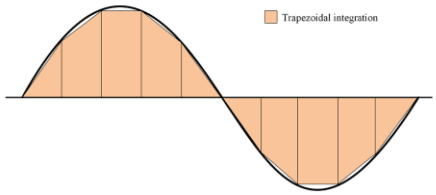

Figure 6
Graphic representation of the trapezoidal integration method

If the velocity is plotted at this point, the response shown in Figure 7 is obtained.

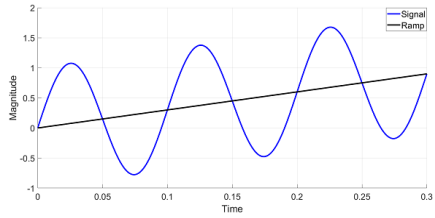

Figure 7
Velocity obtained by direct trapezoidal integration

Note that the resulted integral shown in Figure 7 contains a sinusoidal signal mounted on a ramp. Considering the nature of the movement of the machine, the velocity is expected to have a sinusoidal shape with similar peak values. This implies that the ramp observed in Figure 7 is derived from an integrated offset error associated with the imprecision in the acceleration data. In order to eliminate this ramp, steps 3 and 4 are applied to the signal obtained in Step 2.

Step 3. Peak detection. During a sensor scan window, the first and last peak values contained in the resulting vector of Step 2 are identified and the slope m^v is obtained by dividing the difference in the speed values *Av* by the difference in the time values *At*, i.e., $m^v = Av/At$. Graphically this implies the representation shown in Figure 8.

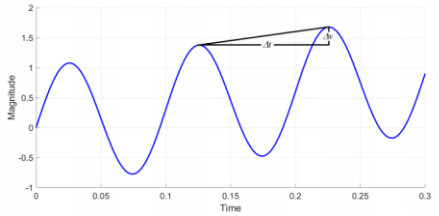

Figure 8
Peak detection of the acceleration integral signal

Step 4. Correction of the offset error. The value of the slope m^v is a linear function proportional to time on the velocity graph $m^v(t) + b$, where the constant part b is still unknown. However, by deriving $m^v(t) + b$ with respect to time, the value m^v represents the offset error in the acceleration data. Then, m^v is subtracted from the acceleration vector obtained in Eq. 1 as shown in Eq. (3).

$$aX[i] = aX[i] - m^v, \ \forall i = 0, \ldots, 255 \tag{3}$$

After this offset correction, step 2 is repeated, obtaining in this case the speed vector without the ramp offset.

Step 5. Remove continuous speed offset. Once the corrected speed is obtained, the constant component *b* from the equation $m^v(t) + b$ is eliminated. In order to achieve this, the maximum and minimum values in the velocity vector are obtained and the value of *b* is derived from the average of these 2 values as shown in Eq. (4).

$$b = \frac{max\{vX\}+min\{vX\}}{2} \tag{4}$$

Then, the velocity vector offset is corrected by subtracting the value of *b*, as shown in Eq. (5).

$$vX[i] \; = \; vX[i] — \; b, Vi \; = \; 0, \ldots, 255 \tag{5}$$

Step 6. Frequency calculation. Taking advantage of the peak detection performed at Step 3, the *At* is divided between the number of peaks *np* found in the velocity vector minus one, to obtain the period and the machine frequency *f* as shown in Eq. (6).

$$\begin{aligned} f &= T^{-1} \\ T &= \Delta t/(np-1) \end{aligned} \tag{6}$$

Step 7. Stroke calculation. Starting from the corrected velocity vector, steps 2 to 5 are now applied in order to integrate and correct the speed data to obtain a position vector associated with the machine stroke.

The X-axis stroke is calculated as the difference between the maximum and minimum values in the position vector as shown in Eq. (7).

$$strokeX = max\{dX\} - min\{dX\} \tag{7}$$

The ADIS16229 is a two-axis sensor allowing to perform the above-mentioned steps for the data obtained, in the same time window, for the Y-axis and calculate the corresponding stroke by Eq. (8).

$$strokeY = max\{dY\} - min\{dY\} \tag{8}$$

The total stroke, *s*, is finally obtained as the square root of the sum of the squares of the strokes in the X and Y axes as denoted in Eq. (9).

$$s = \sqrt{stokeX^2 + stokeY^2} \tag{9}$$

The process to obtain the frequency and stroke is performed for each of the six ADIS16229 sensors paired to the corresponding ADIS16000 sensor hub and repeated continuously. The latest results of the six sensors are stored in the microcontroller and are readily available to be requested via a serial protocol.

The proposed algorithm is programmed into the ESP32 microcontroller to validate this proposal over a wide range of operating conditions using a testbench system. Once the algorithm is validated it can be programmed into the selected Allen Bradley PLC to be installed in the industrial plant.

4 Validation Testbench

The vibrating conveyor machine, to which the proposed fault detection system is applied, has a nominal stroke of 25.4 mm with a nominal vibration frequency of 10 Hz. Within this context, a test bench system capable to operate at different strokes and frequencies around the nominal conveyor parameters is necessary to validate the proposed algorithm.

4.1 Design Requirements

It is desired that the test system has a variable stroke in a range of 20 to 30 mm so that the 25.4 mm nominal conveyor stroke is within this range being possible to emulate larger and shorter strokes. Note that the stroke should have a trajectory as linear as possible to resemble the actual movement of the conveyor.

On the other hand, the vibration frequency that the test system can generate must be in a range of 5 to 20 Hz to emulate the 10 Hz nominal frequency of the conveyor, having a test range from half to twice this nominal frequency.

4.2 Testbench System

Based on the mentioned requirements, the test bench system consists of a 1.2 m long A36 steel arm attached, at one end, to a pair of bearing blocks while the other end is attached to a connecting rod designed to achieve a 30 mm stroke.

This connecting rod is attached to a crankshaft and the latter is held by two bearing blocks with a 500 V-belt pulley attached to its opposite end.

Aligned to the 500 pulley a 4-pole, 60 Hz, three-phase, 3 HP motor with a 1.7500 V-belt pulley on its shaft is placed. Then, a type B model B30 belt is used to transmit the mechanical torque from the 1.7500 pulley in the motor to the pulley in the crankshaft. In this case, the motor speed is controlled by a Power Flex 523 variable frequency drive to obtain the desired vibration frequency.

Note that the 1.2 m arm has a leverage movement such that a range of 0 to 30 mm can be obtained along the arm length. Moreover, the pulleys configuration is designed to obtain a vibration frequency of 10 Hz when the motor voltage has a frequency of 60 Hz. Figure 9 shows a photograph of the test bench system used to validate the proposed algorithm.

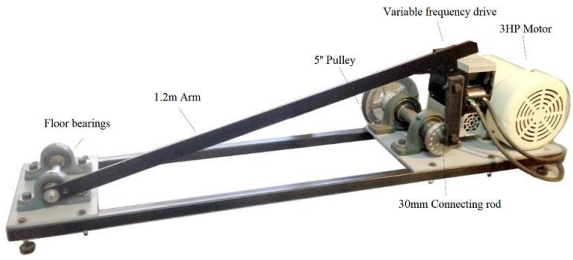

Figure 9
Testbench system

4.2 Prototype

The ADIS16000, which works as the receiver hub, is connected to the SPI port to the ESP32 microcontroller in which the proposed algorithm is implemented. The microcontroller is Wi-Fi connected to a computer to send the data obtained with the proposed method. This data is post-processed in the computer to obtain the mean and variance of each sensor.

Figure 11 shows the complete box containing the microcontroller and the ADIS16000 receiver node with the wireless communication antenna.

Figure 11
ADIS16000 and microcontroller box

Considering that the conveyor machine and the testbench arm are made of carbon steel, the sensor fixing is done using magnets. In this case, seven N50 grade neodymium blocks of 25x10x5 mm are inserted in the base of each sensor node box to achieve the necessary magnetic force to withstand the vibration.

5 Fault Detection Stage

Based on the experience of conveyor maintenance technicians, the operating state of the machine is considered within 3 possible regions: a green safe state, a yellow warning state and a red fault state. In this context, three-color led tower lights,

shown in Figure 9, one for each sensor, are installed near the vibration conveyor machine to continuously indicate to the operator about the stroke and frequency status of the machine.

Figure 9
Three-color led tower light

Table 1 shows the colors associated with the stroke and the frequency status according to the stroke deviation and the frequency deviation, respectively.

Table 1
Contains the result of comparing in pairs with the final result

	Green	Yellow	Red
s^{dev}	< 1 mm	1-2 mm	> 2 mm
f^{dev}	< 0.25 Hz	0.25-0.5 Hz	> 0.5 Hz

This information can be simultaneously sent to a remote location thanks to the IoT capabilities of the ESP32 microcontroller.

The stroke deviation s^{dev} is obtained as the absolute difference between the calculated stroke and the machine nominal stroke s^{nom} according to Eq. (10).

$$s^{dev} = |s - s^{nom}| \tag{10}$$

The frequency deviation f^{dev} is obtained according to Eq. (11) where f^{nom} is the nominal frequency of the machine.

$$f^{dev} = |f - f^{nom}| \tag{11}$$

If both parameters are in the safe state, the green light is ON. If a warning or fault state is presented, the yellow or red lights, respectively, start to blink. The led light blinks at 1 *Hz* to indicate the non-safe state of the stroke, while blinking at 3 *Hz* indicates a non-safe state of the frequency.

If both parameters have a similar non-safe status, the light blinks at 1 *Hz* for 2 seconds, after, the light blinks at 3 *Hz* for 2 seconds and the cycle is repeated. Thus, the operator is visually informed every 4 seconds about the machine status at each sensor location.

Moreover, the led tower contains a buzzer that can be wired together with the red light to have an audible alarm in the case where the stroke or the frequency presents a faulty status.

6 Results and Discussion

6.1 Frequency and Stroke Calculation Validation

Using the testbench system presented in Figure 9, several experiments were performed using different strokes at different frequencies to validate the proposed algorithm.

In order to set the desired stroke, the dial indicator shown in Figure 12 is used to find, with high precision, the point along the arm where the sensor should be placed. This is considering the location of the MEMS accelerometer in the sensor board.

Figure 12
Dial gauge calibration for 25.4 mm stroke.

On the other hand, the PowerFlex variable speed drive is used to obtain the desired frequency, which is measured with a digital stroboscope tachometer.

After testing the strokes in the range of 20 to 30 mm, the results indicated that the algorithm has the highest error in determining the stroke when it is at its maximum value.

Figure 13 shows the estimated strokes obtained with the proposed method for each of the 6 sensors during 10 consecutive scans using a 30 mm stroke and a vibration frequency of 10 Hz.

As can be seen in Figure 13, the S2 sensor estimates have the biggest errors, varying from 28.9 to 29.2 mm. On the other hand, the S1 sensor showed the best estimates, between 29.6 and 29.9 mm.

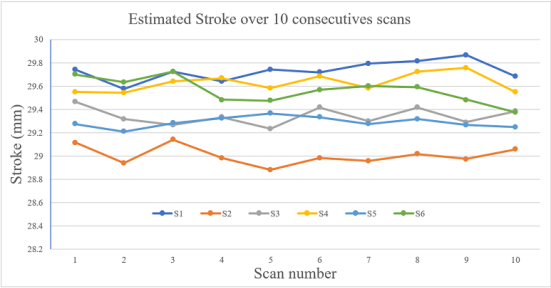

Figure 13
Stroke estimations on the 6 sensors

In order to reduce the errors in the stroke estimates, improving the estimation accuracy, a moving average filter of 10 samples is applied. Considering over one thousand strokes estimated at 30 mm and using the average filter, the mean value, μ, and the standard deviation, σ, of each sensor are obtained and presented in Table 2.

Table 2
Sensor mean values and standard deviations for a 30 mm stroke

	S1	S2	S3	S4	S5	S6
μ(mm)	29.730	29.006	29.343	29.628	29.290	29.563
σ(mm)	0.051	0.055	0.049	0.052	0.053	0.048

To determine if the sensor errors are constant or proportional, the same experiment is repeated for a 20 *mm* stroke. Comparing the sensor mean values for a 30 *mm* stroke with those obtained at 20 *mm*, it was observed a proportional relation such that the correction factors presented in Table 3 were obtained in order to correct the sensor gain that affects the strokes estimates.

Table 3
Correction factor for each sensor

S1	S2	S3	S4	S5	S6
1.0091	1.0343	1.0224	1.0125	1.0242	1.0148

These correction factors *cf* are simply considered in the stroke estimates as denoted in Eq. (12).

$$s = cf\sqrt{strokeX^2 + strokeY^2} \quad (12)$$

By using the correction factors, the stroke estimation accuracy is increased and combined with the sensor precision associated with the corresponding standard deviation, presented in Table 2, the fault detection in the machine stroke becomes attainable.

In the case of the frequency estimation, the proposed algorithm presents good results in the six sensors. Table 4 shows the maximum errors found in the frequency estimates at 10 Hz for each of the 6 sensors.

Table 4

Maximum errors in frequency estimates (Hz) at $10Hz$

S1	S2	S3	S4	S5	S6
0.03	0.04	0.03	0.04	0.04	0.05

As can be seen in Table 4, the proposed algorithm is capable to estimate vibrating frequencies within a precision of ±0.05 Hz, making it suitable to detect failures associated with the vibration frequency in the conveyor machine.

6.2 Fault Detection System Validation

Considering the fault conditions presented in Table 1, different experiments were performed to determine if the proposed fault detection algorithm was able to adequately detect the conveyor machine strokes under different operating conditions.

336 estimations were performed on each sensor operating with a stroke of 1 inch (25.4 mm), the estimations of the sensor with the worst performance were plotted in a histogram and compared to a Gaussian fit to quantify the number of outliers in the case of assuming a Gaussian distribution. These results are presented in Figure 14 where it can be observed that 8 estimations of the 336 performed are outside of the Gaussian assumption.

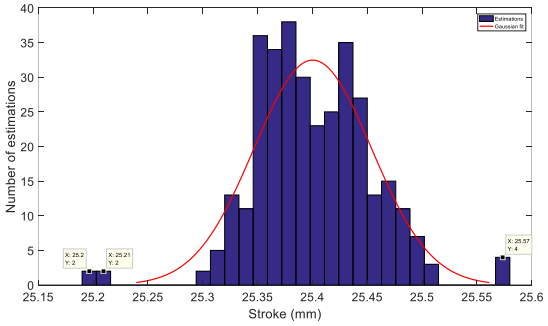

Figure 14

Histogram of estimations from sensor 2

The Gaussian distribution parameters obtained with Matlab representing the red line in Figure 14 have a mean value of 25.4003 and a standard deviation of 0.0536491.

In this context, the fault detection accuracy (FDA) of the proposed algorithm when the stroke deviation is over 2 mm representing the detected faulty red status and

considering a tolerance of ±0.107 mm, corresponding to 2 times the expected standard deviation, is obtained as:

$$FDA = \frac{estimations\ inside\ tolerance}{total\ number\ of\ estimations} 100\% = \frac{336-8}{336} 100\% = 97.62\% \quad (13)$$

The obtained results are compared to the fault recognition accuracy for a belt conveyor based on Support Vector Machine and Grey Wolf Optimization presented in [14] and shown in Table 5.

Table 5

Fault detection accuracy

Method	Accuray (%)
Proposed 7-step algorithm	97.62
Support Vector Machine and Grey Wolf Optimization	97.22

Conclusions

A reliable method to obtain stroke and frequency data derived from the G-force measured by a vibration sensor is presented. This method is able to define in a non-invasive way the operating state of the machine allowing the operators to program preventive maintenance with greater efficiency.

Based on the test system specifically designed and built to test the proposed methodology, it was possible to corroborate the precision of the method and the reliability that it can offer in its application in the industrial field.

It was also possible to define a methodology to obtain correction factors for the stroke and to be able to calibrate the sensors because due to the nature of their construction they present small differences in their sensitivity.

It is worth mentioning that the acceleration sensors were selected based on their availability in the development stage; however, the proposed methodology can be easily implemented using any two-axis acceleration sensors with similar characteristics.

The conveyor machine was validated in a 30-mm wide range, such that the developed system is useful for similar applications in this range, and can be easily modified to be adapted to different ranges.

The fault detection system was validated under fault conditions in a physical testbench obtaining a detection accuracy of 98.01%.

Finally, the selected ESP32 microcontroller allows not only the implementation of the developed 7-step algorithm adequately but including IoT capabilities to the system such as remote monitoring and alarm notification.

References

[1] L. O. Freitas, P. R. Henriques, P. Novais, Analysis of human activities and identification of uncertain situations in context-aware systems, International Journal of Artificial Intelligence, Vol. 18, No. 2, 2020, pp. 135-154

[2] C.Andreeski, D. Mechkaroska, Modelling, forecasting and testing decisions for seasonal time series in tourism, Acta Polytechnica Hungarica, Vol. 17, No. 10, 2020, pp. 149-171

[3] R. E. Precup, T. A. Teban, A. Albu, A. B. Borlea, I. A. Zamfirache, E. M. Petriu, Evolving fuzzy models for prosthetic hand myoelectric-based control (IEEE Trans. Instrum. Meas. 69(7), 2020, pp. 4625-4636

[4] M. Devaney, L. Eren, Detecting motor bearing faults, IEEE Instrumentation and Measurement Magazine 7 (4), 2004, pp. 30-50

[5] X. Gong, X. Ma, Y. Zhang, J. Yang, Application of fuzzy neural network in fault diagnosis for scraper conveyor vibration, in: 2013 IEEE International Conference on Information and Automation (ICIA), IEEE, 2013, pp. 1135-1140

[6] I. El-Thalji, E. Jantunen, A summary of fault modelling and predictive health monitoring of rolling element bearings, Mechanical Systems and Signal Processing 60, 2015, pp. 252-272

[7] M. Gajowy, Operational properties of vibratory conveyors of the antiresonance type, in: 2019 20th International Carpathian Control Conference (ICCC) IEEE, 2019, pp. 1-7

[8] G. Zak, A. Wylomanska, R. Zimroz, Local damage detection method based on distribution distances applied to time-frequency map of vibration signal, Proceedings of the 2017 IEEE 11th International Symposium on Diagnostics for Electrical Machines, Power Electronics and Drives, SDEMPED 2017 2017-Janua (5), 2017, pp. 134-140

[9] P. Misra, D. Roy, T. Chakravarty, A. Pal, Unobtrusive vibration sensing using optical strobing: Performance analysis, Proceedings of the International Conference on Sensing Technology, ICST 2017-Decem, 2018), pp. 1-4

[10] K. Kuribayashi, R. Nagase, S. Wada, L. Kobayashi, Study of vibration sensing technique using Fabry-Perot interferometer with optical fibers, IECON Proceedings (Industrial Electronics Conference) 2019-Octob, 2019, pp. 7143-7147

[11] Z. Liao, P. Chen, A Vibration Signal Filtering Method Based on KL Divergence Genetic Algorithm-With Application to Low-Speed Bearing Fault Diagnosis, International Conference on Digital Signal Processing, DSP 2018-Novem, 2019, pp. 7-11

[12] C. Kinergy, Induced Conveying (1997) URL https://www.kinergy.com/induced conveying

[13] H. R. Holmes, K. F. B¨ohringer, Vibration induced transport of enclosed droplets, Micromachines 10 (1), 2019, p. 69

[14] X. Li, Y. Li, Y. Zhang, F. Liu, Y. Fang, Fault Diagnosis of Belt Conveyor Based on Support Vector Machine and Grey Wolf Optimization, Mathematical Problems in Engineering, Vol. 2020, 2020, pp. 1-10